SOME PRACTICAL ASPECTS OF ELECTROMAGNETIC ACTIVATION

CHRISTOPHER MACLEOD[1], KENNETH S. GOW[1] AND NICCOLO F. CAPANNI[2]
1. *School of Engineering, The Robert Gordon University, Aberdeen, AB10 1FR, UK.*
2. *School of Computing, The Robert Gordon University, Aberdeen, AB10 1FR, UK.*

Electromagnetic Activation (EMA) is an alternative to combustion in Scramjet-like hypersonic engines. The basis of the system was outlined in previous publications. This paper builds on these results and explores some further practical and theoretical aspects of its operation. These include the beam paths and thermodynamics of the duct, the efficiency of the system, a review of the available radiation generation devices and a discussion of power supply options.

Keywords: Scramjet, electromagnetic activation, hypersonic ducts

1. INTRODUCTION

The idea behind Electromagnetic Activation (EMA) was outlined in the paper *Electromagnetically Activated Hypersonic Ducts* originally published in *JBIS* [1]. The paper proposes the use of heat generated by the absorption of Electromagnetic Radiation as an alternative to that produced by combustion in Scramjet-like engines. A short description of the system is given in section 2.

For reasons of space, not all aspects of the method were covered in the original paper. Interesting questions about the practical implementation were also raised by the reviewers. The purpose of this paper is to address these issues and to further extend the theoretical basis of the system. It is hoped that this discussion, together with that outlined in the original paper, will form a body of work which will allow further design studies and in particular, experimental verification and development to take place.

The original paper outlined the use of both Millimetre Wave and Ultraviolet Radiation in the duct. This paper, however, will confine its discussion to the Millimetre Wave version. Although the Ultraviolet has some advantages over the Millimetre Wave system, they are currently outweighed by the practical disadvantages. These are principally the lack of suitable window materials and efficient and powerful emitters. The behaviour of the Ultraviolet system is also more difficult to predict theoretically because it relies on electron energy activation, rather than rotational energy, as in the Millimetre version.

2. REVIEW OF OPERATION

The principle idea behind EMA is shown in Fig. 1. Instead of fuel being injected into the air-stream and burnt, as is the case in a normal Scram system, the flow is instead heated by Electromagnetic Radiation emitted into the stream and absorbed by it. This radiation directly activates the stream at the molecular level, coupling to its rotational, translational, vibrational or electronic energy modes. When EMA is used to heat air in a hypersonic duct in this way, the resulting system may be termed an Electromagnetically Activated Hypersonic Duct or EMAHD.

The principle advantages of this approach are: Because the flow is directly activated by an effect travelling at the speed of light, most of the problems associated with mixing and flame-holding present in Scramjets, are mitigated. Further, the duct can be mechanically continuous, with no injectors or added fuel to disrupt the flow. Finally, because the conditions in the duct do not have to support combustion, a wider range of pressures and temperatures can be tolerated. The principle (and critical) disadvantage is the power requirement.

The absorption of radiation in the duct is given by the Beer-Lambert Law. It was shown in the original paper, that the distance x required to absorb a particular proportion of the radiation was given by.

$$x = \frac{\ln\left(1 - \frac{P}{100}\right)}{-(\sigma n)} \quad (1)$$

Where P is the percentage of radiation to be absorbed. In most of the examples given, this figure was 99% - meaning x is the distance required to absorb 99% of the power of the initial radiation. The symbol σ is the Absorption Cross Section of the species involved, usually specified in cm^2 (in which case x is in cm) and n is the number density of the species in particles per cm^3.

If long pathlengths are required for absorption, the radiation propagates in the duct by wall reflection in a similar way to radiation propagating along a waveguide. In this way, very long pathlengths can be accommodated. It was shown that the required duct length D of a parallel sided duct is given by.

$$D = L \sin \theta \quad (2)$$

Where L is the required radiation pathlength and θ is the launch angle measured from a normal to the duct wall. In most cases, the distance x calculated in equation 1, is the radiation pathlength L in equation 2.

For the reasons mentioned in the introduction, this paper
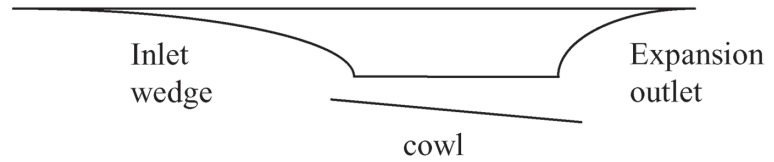
Typical Scramjet layout

Fig.1 A comparison of EMA and normal Supersonic Combustion.

EMA   *Supersonic combustion*
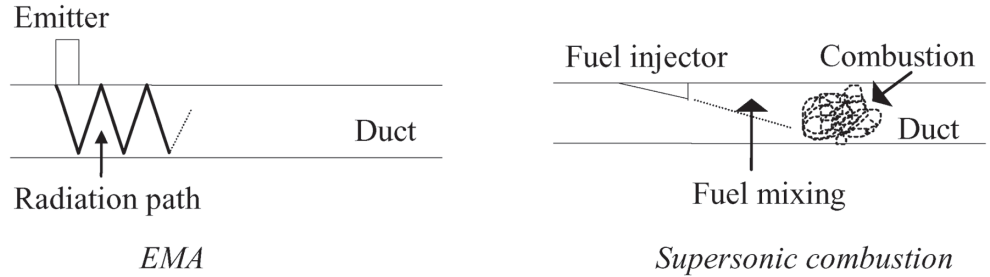
will concern itself with the millimetre wave version of the system. The region is centred around 61GHz, where the magnetic moment of molecular oxygen is strongly absorbing.

Using published data for the temperatures, pressures and densities in the duct of a well-known and fairly typical Scramjet design by Billig [2] and discussed by Anderson [3], the required radiation pathlengths were calculated, as shown in Table 1.

The final column of Table 1 gives the worst-case conditions usually quoted for combustion - an air density of 0.5 atm and a temperature of 2000K. The Billig data will also serve as a discussion point for this paper.

The rest of this paper details some of the practical and theoretical issues involved with this system that were not outlined in the original paper. Some of these issues were raised by engineers reading the paper, some by the original reviewers and some by the authors themselves. They mainly involve questions about the practicality of the system, the availability of suitable generating devices, the efficiency of the duct and the generalisation of some of the results from the original paper.

3. SHAPING RADIATION PATHS WITHIN THE DUCT

In the original EMA paper [1], the relationship between pathlength and duct-length was developed and resulted in the derivation of equation 2. This equation gives the duct-length required to accommodate a given radiation path-length in a parallel-walled duct. Diverging ducts are generally not practical, this is because, at any angle of wall divergence great enough to give a measurable aerodynamic effect, the angle of the incident beam rapidly increases until, after only a few reflections, the beam exits the structure, as shown in Fig. 2. Further, in a converging duct, the angle of incidence rapidly decreases until it passes through the normal to the duct wall; whereupon the beam changes direction, and the structure becomes a diverging duct - with the effect just described.
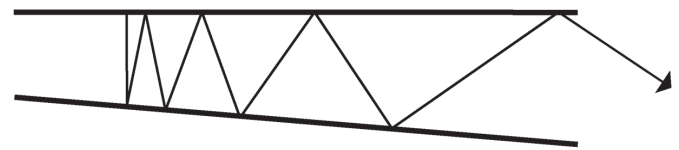

Fig. 2 Reflection angle in a diverging duct.

Beam paths may be controlled and shaped using dielectric-windowed mirrors. The material nature of these is explored in section 5.2; in this section the radiation path is described. The simplest case is when a mirror is used to change the direction of a beam - for example, to reflect it back into the active volume of the duct so that long path-lengths can be accommodated in shorter duct-lengths. Figure 3 shows this situation.

This situation can be analysed by considering the incident and reflected rays as shown in Fig. 4.

Consider first, Fig. 4a. There is a right angled triangle formed by points b, c and d.

$$\delta = 90 - \Omega \qquad (3)$$

Now consider angles δ, α and γ at point c.

$$\gamma + \alpha + \delta = 90 \qquad (4)$$

Substituting equation 3 into 4.

$$\gamma + \alpha + (90 - \Omega) = 90$$
$$\Rightarrow \gamma = \Omega - \alpha$$

Now taking the second diagram and considering the triangle formed by points c, d and h.

$$\phi = 90 - \Omega + \gamma$$
$$\text{now } \phi + \eta = 180$$
$$\text{so } \eta = 90 + \Omega - \gamma$$

TABLE 1: *Pathlengths Required at 61GHz for 99% Absorption of Power.*

Mach	7	10	15	20	0.5atm, 2000K
Number density n of O_2 (#/cm³)	2.35×10^{18}	1.64×10^{18}	9.97×10^{17}	4.33×10^{17}	3.57×10^{17}
Pathlength (km)	2.8	4.0	6.5	15.0	18.1

Fig. 3 Using a windowed mirror to control beam path.
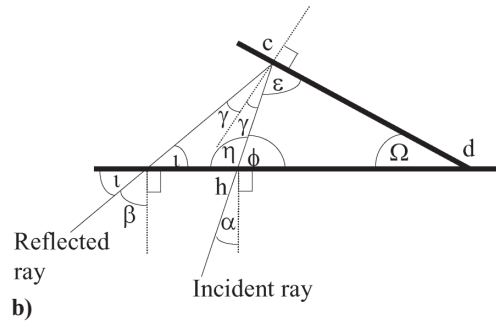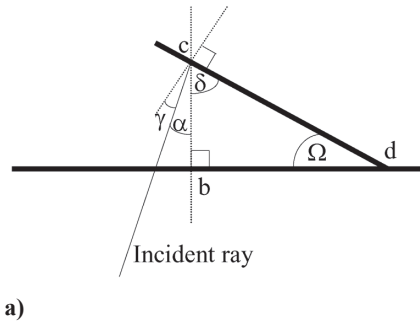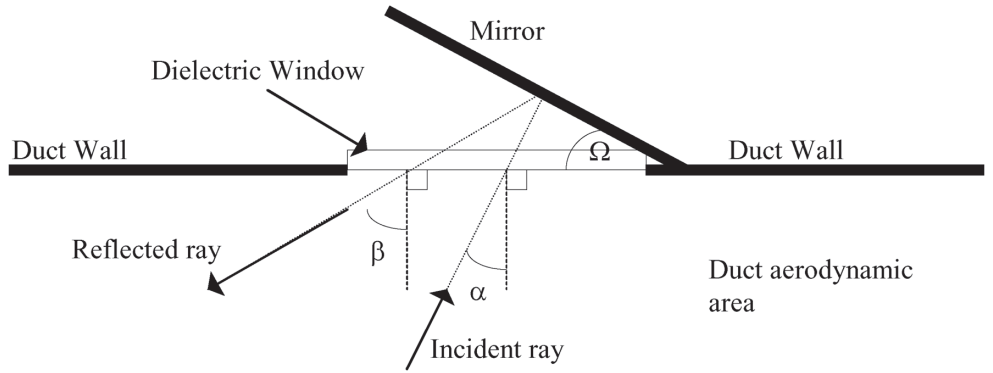
Fig. 4 Geometrical constructs of reflecting mirrors.

a)

b)

Next, consider triangle formed by angles ι, η and 2γ.

$$\iota = 90 - \Omega - \gamma$$

$$\text{but } \beta = 90 - \iota$$

$$\therefore \beta = \Omega + \gamma$$

So to find β in terms of Ω and α.

$$\beta = \Omega + \gamma$$

$$\text{but } \gamma = \Omega - \alpha$$

$$\therefore \beta = \Omega + (\Omega - \alpha)$$

and

$$\beta = 2\Omega - \alpha \qquad (5)$$

This last equation (5) gives the reflected ray angle in terms of the incident ray angle and the angle of the mirror. The efficiency of these systems is discussed in section 5. It should be noted however, that there may be other practical options for reflection, for example Dielectric based reflectors or cavity mirrors.

The same idea also lends itself to more complex topologies designed to control the width and divergence of the beam, Fig. 5.

In this crude illustrative case, the emitter, radiating a cone-shaped beam pattern, is placed at the focus of a convex reflector, which collimates the beam. Obviously different shapes of reflector may be introduced to achieve different results, depending on the required beam-profile. The shapes used will be carefully selected for their purpose using computer-aided ray-tracing mirror design and are too multifarious to pursue further here.

4. TEMPERATURE RISE WITHIN THE DUCT

In systems operating in rarefied atmospheres, the mode of heat transfer depends on whether the gas can be treated as a con-
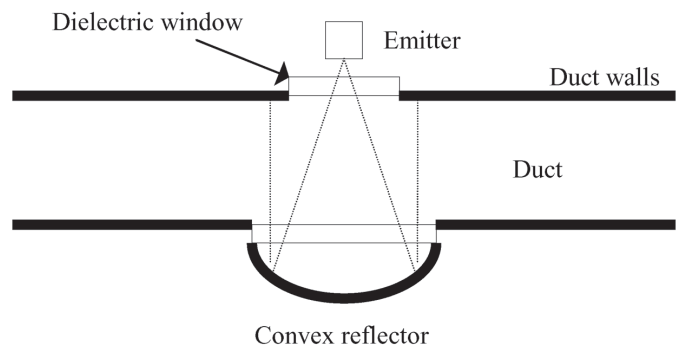
Fig. 5 Typical collimating arrangement.

tinuum or whether the Mean Free Path is large enough so that free molecular effects cannot be ignored. This distinction is made using the Knudsen Number - which is the ratio of the Mean Free Path to the Characteristic Length of the engine [4].

The Knudsen number can be stated in various ways, depending on the situation at hand. In this case, probably the most relevant formulation is.

$$\text{At } Re > 1, \text{ continuum flow exists if } \frac{M}{\sqrt{Re}} < 0.01$$

$$\text{At } Re < 1, \text{ continuum flow exists if } \frac{M}{Re} < 0.01$$

Where Re is the Reynolds Number and M is the Mach Number [4]. These values may be calculated for Billig's data as shown in Table 2.

The table indicates that the flow may be treated as a continuum in this case. This conclusion is supported by other examples in the literature [5]. In the case of EMA, because the flow is activated directly at the molecular level, many of the effects associated with heat transfer in rarefied gases would be mitigated anyway. This may be important, as the technique can still operate in flows at lower pressures

TABLE: 2 *The Nature of Flow Through the Duct.*

Speed	ρ (kg/m³)	Speed (m/s)	Re	M/√Re	Continuum
Mach 7	0.563	3984	3.96 x 10⁸	0.0004	Yes
Mach 10	0.390	6504	4.48 x 10⁸	0.0004	Yes
Mach 15	0.238	12027	8.59 x 10⁸	0.0005	Yes
Mach 20	0.105	19071	6.00 x 10⁸	0.0008	Yes

than for combustion systems - one way of handling this and still use the equations presented below, is to modify the value used for Specific Heat Capacity, to take the low molecular collision rate into account.

Having established that continuum flow conditions apply, the temperature rise [6] in a mass of gas m_g due to added energy E is.

$$\Delta T = \frac{E}{Cm_g}$$

Where C is the Specific Heat Capacity of the gas. This of course assumes an adiabatic system, which given the nature of the flow, is generally a good first approximation [5].

In terms of radiation entering the duct, it is easier to work with power rather than energy and since $P = E/t$, taking the instantaneous case.

$$\frac{dT}{dt} = \frac{P}{Cm_g}$$

The mass here is that coincident with the volume of the beam. In other words.

$$m_g = \rho \text{ x } beam\_volume$$

Where ρ is the gas density. The volume of the beam is its cross-sectional area multiplied by the path-length. The path-length is denoted L in equation 2. This equation, and the others previously presented, assumes a parallel beam and uniform density over the active volume. In practice, these might vary and an alternative value may have to be calculated using integral calculus or summed discrete values. The exact formulation of this will depend on the topology of the system used. However, the simple case is still likely to be the most common; it is also the most instructive and may be used for rough calculations even in more complex situations.

The approach above allows the formulation of the equation in terms of more appropriate parameters. If the beam cross sectional area is denoted B, then.

$$\frac{dT}{dt} = \frac{P}{C\rho LB}$$

For a small parcel of air passing through the duct, the final temperature reached will depend on its time in the beam active volume. This may be calculated from the speed of the airflow v and the active duct-length of the beam - labelled D in equation 2. If v varies, then it must be integrated to find the average value. Since the exposure time is D/v and assuming that the radiation fills the whole volume then.

$$\Delta T = \frac{PD}{C\rho vBL} \tag{6}$$

A possibly more useful way for formulating this is to rewrite it in terms of the duct mass flow rate.

$$P = \frac{dm}{dt}\Delta TC$$

Which can be rearranged to give the temperature rise for a given mass flow rate and absorbed power.

$$\Delta T = \frac{P}{\dot{m}C} \tag{7}$$

The mass flow rate may be calculated from $Av\rho$ (where A is the cross-sectional area of the duct). This equation is useful because it allows the calculation of the fundamental duct aerodynamic parameters. In particular, it gives the flow-rate required in order to produce a particular temperature rise for a known power input.

A detailed example is not included here, as published Scramjet designs like that of Billig are based on the pressure, temperature and density ratios required for combustion. Although these are often useful for fluid flow figures, they are not necessary typical of the thermodynamic parameters in an EMA system. However, as an approximate guide, many published designs have a mass flow rate of between 5 and 50 Kg/m³. Taking an (again typical) temperature increase of 1500K gives, from equation 7, a required absorbed power from approximately 5 MW (for the lower mass flow rate) to 50 MW (for the upper).

5. LOSSES AND EFFICIENCY

The efficiency of an EMAHD propulsion system, as shown in Fig. 6, can be divided into the efficiency of the power-supply system, including the connection to the radiation generator device (labelled (a) in the diagram); the efficiency of the device and its associated feed to the duct (b) and the efficiency of the duct itself. These duct losses may be due to radiation losses (c) or to the thermodynamic and fluid efficiency of the duct (d).

The losses in the power-supply system are strongly dependent on the nature of that system, which, as discussed in section 7, may be one of several different choices. Because of this, the efficiency of the power-supply will not be discussed further here. A large body of published data is available on the efficiency of the radiation generator system and this will be discussed in section 6. The aero-thermodynamic losses are discussed in detail in other work [5, 7] and so are not covered in this paper.

This section will therefore confine itself to the losses unique to EMA - the Millimetre Wave losses in the duct itself (item (c) in Fig. 6). These losses are illustrated in Fig. 7.

Fig. 6 Losses in a complete propulsion system.

Losses in electrical power supply system (a)

Losses in radiation generator (b)

Millimetre wave losses in duct (c)

Aero-thermodynamic losses in duct (d)

Available power from store

Contribution to thrust

Window losses

Reflection losses

Losses due to duct contamination and imperfections

Available power from radiation input feed
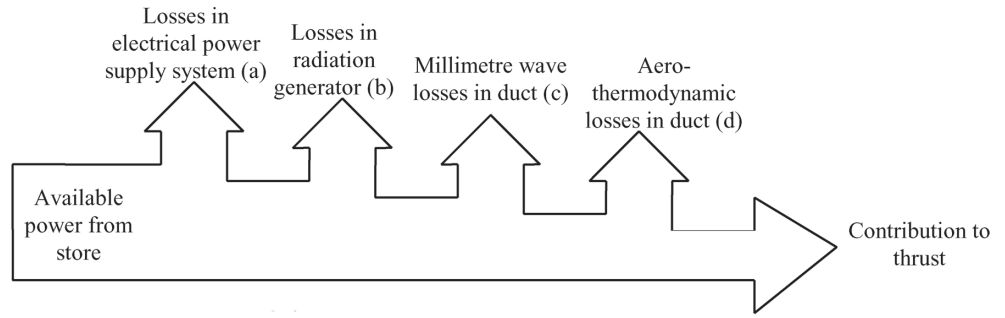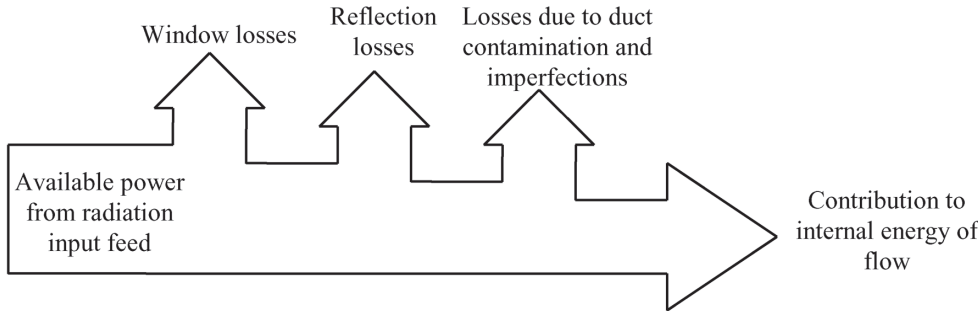
Contribution to internal energy of flow

Fig. 7 Millimeter-Wave Losses in the duct.

The sections below consider these losses in order of their magnitude and make estimates of their importance and influence on system design.

5.1 Reflection Losses

The largest losses in the duct system will be due to energy being absorbed in the duct walls. Only a perfect conductor can reflect radiation with no losses. Real conductors, by virtue of their resistance, absorb some radiation. This absorbed energy manifests itself as heating of the conductor. The incident energy only penetrates a short way into the conductor - a distance known as the skin-depth. The absorption is governed, therefore, by the resistivity of the material involved. The resistivity of several important metals, commonly used in alloys, and their temperature coefficients are shown in Table 3.

TABLE 3: *Resistivities of Some Important Metals.*

Material	Resistivity (Ωm x 10^{-8}) at 20°C	Temperature Coefficient (°C^{-1})
Silver	1.59	0.0038
Copper	1.72	0.0039
Aluminum	2.82	0.0039
Tungsten	5.6	0.0045
Nickel	6.99	0.0057
Iron	10	0.005

As can be seen from the table, Silver is the most conductive metal (in fact, the most conductive electrically and thermally of all metals) and unfortunately, Iron is a rather poor conductor. These figures will have a major impact on reflection losses.

The reflection of plane waves from a metal is treated in any standard text on electromagnetics [8]. The reflected power is given by the square of the reflection coefficient.

$$|\rho|^2 \approx 1 - \frac{4R_s}{\eta}$$

The second term represents the approximate power loss in the conductor (the exact expression is an infinite power series).

$$Loss \approx \frac{4R_s}{\eta}$$

Where R_s is the surface resistance and η is the impedance of the transmitting medium (in the case of the duct, the impedance of free space, 377Ω). The surface resistivity can be found from the conductivity and skin-depth of the material at the frequency of interest by.

$$R_s = \frac{1}{\delta\sigma}$$

Where σ if the conductivity in Siemens per meter and δ is the skin-depth in meters. The skin-depth is a function of the electrical properties of the material and the frequency of interest.

$$\delta = \frac{1}{\sqrt{\pi f \mu\sigma}}$$

Where f is the frequency and μ is the permeability of the conductor material in Henrys per metre. The skin-depth and therefore loss increases with frequency [8].

This information now allows the calculation of the loss on reflection at 61GHz. These losses are tabulated in Table 4 for four conductors: Silver, the best conductor; Copper, a very good conductor; Aluminum, a reasonable conductor and a typical Brass, a rather poorer conductor. The figures are given for conductors at 20°C.

The absorption of radiation, due to the intervening gas, in one crossing of the duct, can be calculated from the Beer-Lambert Law.

$$I = I_o e^{-\alpha x}$$

Where I_o is the intensity of radiation entering the path, I is the intensity at distance x in the medium (in this case, the distance between reflections) and α is the Absorption Coefficient. One way of increasing absorption is to design the duct to have as high a number-density of absorbing particles as possi-

TABLE 4: *Percentage Loss per Reflection from Common Conductors at 61GHz.*

Material	σ (s/m)	δ (m)	R_s (Ω)	% power loss per reflection
Brass	1.57×10^7	5.14×10^{-7}	0.123	0.130
Aluminum	3.72×10^7	3.34×10^{-7}	0.080	0.085
Copper	5.80×10^7	3.67×10^{-7}	0.064	0.068
Silver	6.17×10^7	2.56×10^{-7}	0.062	0.065

ble - although there is a trade off between this and a high temperature in the duct.

Knowing both the absorption in one crossing and the loss on reflection, it is now possible to calculate duct percentage power loss due to reflection (which is the percentage ratio of reflection loss to absorption). This is done in Table 5 for path lengths between reflection of 1m, 2 m, 5 m and 10 m. The conductors are at 20°C.

In these figures, percentages greater than 100 mean more power is lost on reflection than in absorption (for example, a figure of 500% means that 5 times more power is lost on reflection, than is absorbed by the flow). These, and the other whole figures in this section, have been rounded up to the nearest whole number, in order to give a conservative view. Figure 8 shows the figures for Aluminium (Al), Copper (Cu) and Silver (Ag) plotted on a graph for path-lengths of 5 m and 10 m.

One can immediately see that for good efficiency, two conditions are necessary. Firstly, long path-lengths between reflections. Secondly, duct walls with high conductance. The first of these conditions suggests ducts with wide mouths, of the type shown in Fig. 9; the radiation is then fired across the duct as shown. The second condition necessitates the use of duct walls of high conductivity material.

The high conductivity requirement presents a number of challenges. Many metals with this attribute are ductile, have a relatively low melting points (copper 1083°C and Silver 961°C) and some also oxidise. However, there are several ways around these issues. Copper is fortunate in being easy to alloy with many useful metals - such as Nickel, Aluminium, Silver and others [9]. Some of these alloys have more appropriate properties than copper itself [10]. A high conductivity liner could therefore be inserted into the duct as illustrated in Fig. 10.

This liner may be thin, because the skin depths involved are very small, as can be seen from Table 4. To avoid oxidation, a passivating thin-film can be sputtered onto the surface. A number of the materials described in section 5.2 are suitable for thin-film deposition like this. A film of alumina (which has a rather poor loss-tangent at these frequencies) 2 μm thick, of this nature, would only increase the loss per reflection of copper by about 2%.

A further complication is introduced because most metals increase their resistance with temperature. For example, a metal sample of resistance R_{ref} at a temperature of T_{ref}, will have a resistance R at temperature T, given by the equation (which is again a power series approximation).

$$R \approx R_{ref}[1 + C(T - T_{ref})]$$

TABLE 5: *Percentage Power Losses due to Reflection Over Various Path Lengths.*

Material	% loss at Mach 7	% loss at Mach 10	% loss at Mach 15	% loss at Mach 20	% loss at 0.5atm/2000K
Path length = 1 m					
Brass	76	112	186	422	487
Aluminum	50	73	122	276	318
Copper	40	59	97	220	255
Silver	39	56	93	211	244
Path length = 2 m					
Brass	40	56	93	211	260
Aluminum	26	37	61	138	175
Copper	21	30	49	111	136
Silver	20	28	47	106	130
Path length = 5 m					
Brass	16	22	37	85	103
Aluminum	11	15	24	56	67
Copper	9	12	20	44	54
Silver	8	12	19	43	52
Path length = 10 m					
Brass	8	12	19	43	49
Aluminum	6	8	13	28	32
Copper	5	6	10	23	26
Silver	4	6	10	22	25

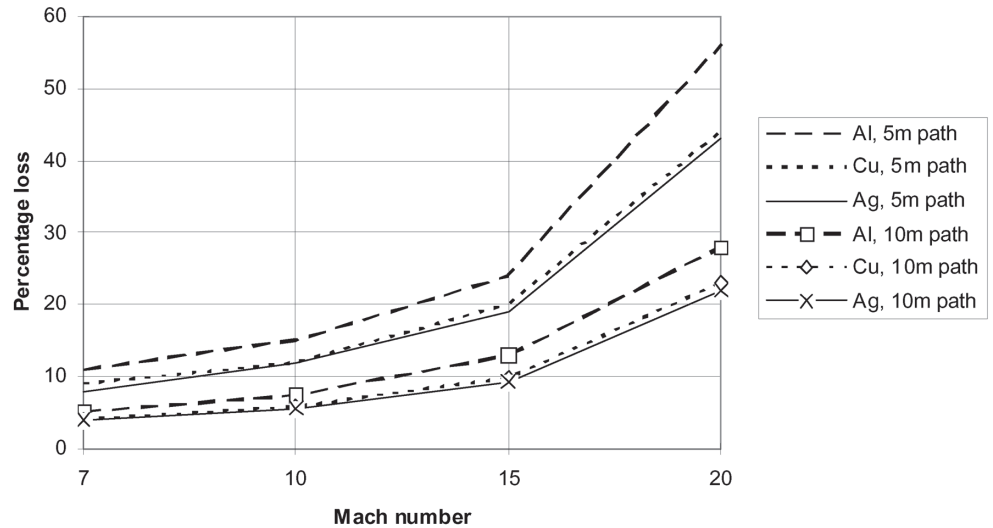**Reflection loss in 5 and 10m path lengths from Mach 7 to 20**

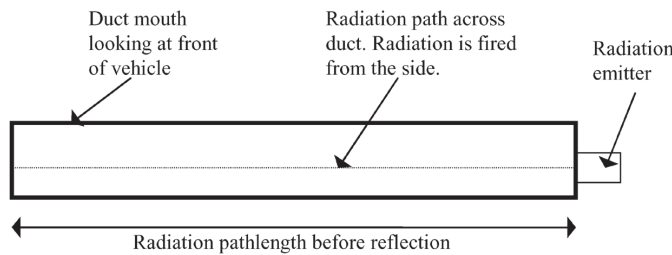**Fig. 8 Losses in 5 m and 10 m ducts for three different conductors**

Fig. 9 Duct shape for long path lengths.

Fig. 10 A duct with a high conductivity liner.

TABLE 6: *Increase in Resistivity with Temperature.*

Material	% increase in resistivity per 100°C
Aluminium	44
Copper	41
Silver	39
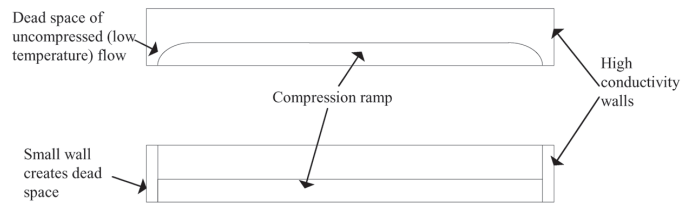
Fig. 11 Design of ducts to minimise reflection losses.

Where *C* is the Temperature Coefficient of Resistance given in Table 3. This means that the resistivity of the walls will increase as shown in Table 6.

Given this consideration, an alternative approach to maintaining low losses is to modify the aerodynamic design of the duct, so that the walls used for reflection remain cool. Figure 11 shows two possible solutions to this. In a), the compression ramp does not extend fully across the duct, leaving a small "dead space" of uncompressed (and therefore cool) flow at the edge. In b) the dead space is generated by masking some of duct space using a side wall.

Active cooling of the walls may also be employed, given the high thermal conductivity of many of the metals (particularly silver). This may involve using cryogenic fuels if available, or perhaps the Peltier effect otherwise.

5.2   Window Losses

After reflection losses, the losses incurred by the Millimeter Wave power traversing dielectric windows represents the next largest radiation loss. This loss, however, is an order of magnitude lower than that described in the previous section - amounting, with good design, to a few percent overall.

A number of different dielectric windows are available for

operation in the Millimeter Wave bands. Many of these are ceramic or crystalline materials, the most popular are shown in Table 7 (note, however, that others, particularly silicon compounds, are also available). The last three materials are not quite so widely used.

Of these materials, not all are characterised in terms of loss-tangent at 61GHz; however, two important ones are: Diamond [11] and Aluminium Oxide (Al_2O_3), commonly called "Alumina" [12, 13]. These are particularly good examples, as diamond is considered to have an extremely low loss-tangent (although possibly bettered by some specialised Silicon materials); Alumina, by contrast, is cheap, but considered to have a fairly poor loss-tangent (although this depends on its purity, and the monocrystalline form, commonly called sapphire, is often a good compromise). The other materials in the table come in-between these two extremes, both in terms of cost and of loss performance.

It is possible to calculate the loss associated with windows made from these materials because if the Loss Tangent is small (much less than unity - which it is, in both cases) then the power out of the window *P* is.

$$P = P_{in}e^{-\delta kx}$$

Where P_{in} is the incident input power, δ is the Loss Angle (because the Loss Tangent is much less than unity, $tan\ \delta \approx \delta$) and *x* is the window thickness.

TABLE 7: *Common Materials for use in Windows.*

Material	Relative Permittivity (F/m)	Melting Point (°C)	Comments
Diamond (C)	10	800	Expensive
Alumina (Al_2O_3)	10	2000	Common and cheap
Sapphire	10	2000	Monocrystalline Al_2O_3
Beryllium Oxide (BeO)	6.7	1900 (max service)	Dust is toxic
Silicon Nitride (Si_3N_4)	7.5	1900 (decomposes)	
Aluminium Nitride (AlN)	8.9	2200	
Titanium Nitride (TiN)	9	2930 (oxidises 600)	

From this relationship, the percentage power losses can be calculated for various thickness of windows, as shown in Table 8.

The extreme thickness of Diamond shown in the table is not of course currently obtainable, but the figures serve to illustrate the likely lower limits of loss accessible. Since it is unlikely that there would be more than about four windows in the beam path, window losses could be kept fairly low as remarked on at the beginning of the section. It should be noted also, that most of these materials can be deposited as thin-films; these, by nature of their thinness, cause only a small loss, while providing a useful protective coating.

Windows do present other practical problems however. In particular localised heating at high powers - although several of those described above are in service as windows for systems with peak powers of hundreds of megawatts. Because of this, windows are sometimes actively cooled. Hot-spots can occur, particularly when a defect or contamination is present in the window. Such considerations lead to it being likely that windows will have to be replaced from time to time. This requirement would be less if multiple emitters were being used (and therefore a lower power density), rather than one large emitter. As will become apparent in later sections, there are other practical reasons why this might be a good strategy.

5.3 Other Duct Losses

Under some circumstances other, smaller, losses may occur from time to time. These may be caused by contamination in the duct. However, this is likely to be minor as, since there is no fuel being burnt in the duct, there are no soot deposits. In addition, the duct is only likely to become active at high altitude - in Billig's design, Mach 7 is reached at an altitude of 25 km. This is well above most of the atmosphere and in particular the troposphere, which contains most of the particulate matter.

Should any organics end up on the duct walls, they are likely to be carbonised quickly by the high radiation density and gas temperature. These carbon deposits could conceivably cause the formation of hotspots in the duct. The losses and therefore heating are difficult to predict because they depend on the extent, composition and nature of the contamination. However a number of papers do examine losses in various types of Carbon deposit [14].

Two other losses are probably worth mentioning. One is scattering by duct irregularities. This is somewhat unlikely in well designed ducts, as the irregularities would have to be of a similar magnitude to the wavelength - which at 61GHz is around 4mm. Obviously through, attention must be paid to the mechanical design and conformance of the duct. The second loss is due to the formation to oxide on the reflector surface. This was alluded to earlier and its effect is unclear as it will vary from material to material. However, keeping the duct cool, choosing the correct alloys and using thin-film protective layers will lessen its effect.

These various effects indicate that the duct and reflector surfaces will require regular maintenance. This will range from regular cleaning and inspection, to the reapplication of protective surfaces and replacement of parts such as windows. The nature and extent of this regime is unclear at the moment and will probably remain so until experimental data is available.

6. RADIATION GENERATION DEVICES

The initial paper on EMA gave a brief overview of Radiation Generators, which was probably rather optimistic in its assessment of their current capabilities. This section reviews the available devices in more detail and considers the development opportunities for newer technologies.

There are basically three high-power generator devices available at microwave and millimeter wave frequencies. These are the Magnetron, the Klystron and the Gyrotron. There are also a number of hybrid devices which are combinations of these three or combinations which use some aspects of lower powered devices like Travelling Wave Tubes.

6.1 Conventional Devices

Magnetrons and Klystrons are familiar devices with outputs at microwave frequencies, producing pulsed powers which extend to hundreds of megawatts. The Klystron, which was invented in the USA, is often the device of choice for plasma heating in fusion experiments. An example of a high powered device for this purpose is the E3712 manufactured by Toshiba, this operates at a frequency of 2.9GHz with a 100MW pulsed output power and a weight of 380kg. A similar continuous-wave klystron is the E3778 device, by the same company,

TABLE 8: *Percentage Power Losses in Diamond and Alumina Windows of Various Thickness.*

Material	Loss Tangent	Loss 0.5 mm	Loss 1 mm	Loss 2 mm	Loss 5 mm	Loss 1 cm
Diamond	1×10^{-5}	0.00064	0.0013	0.002	0.006	0.0128
Alumina	5×10^{-3}	0.319	0.617	1.270	3.144	6.189

delivering 1.4MW. Klystrons are heavy devices, but are capable of more flexible operating modes and greater frequency stability than Magnetrons.

The Magnetron was invented in the UK and is basically a pulsed device. Its frequency stability is less than for a similar Klystron - however, it is lighter and megawatt pulsed-powers are available in devices weighing only a few tens of kilograms - for example the M5028 manufactured by E2V, with an output power of 5MW and a weight of 8 kg. Neither the pulsed nature of the output, nor the lack of frequency stability is necessarily a problem for EMA at 61GHz, where the absorption band is broad [15]. One big advantage of both Klystrons and Magnetrons is that modern devices routinely exceed 60% efficiency and specially designed devices have efficiencies of up to 80%.

Obtaining information on either of these devices' capabilities at 61GHz is difficult. This is for two reasons: Firstly, because of the high atmospheric absorption at these and similar frequencies, they have few applications and there are no high power devices manufactured which have data accessible in the public domain. Secondly, what applications there are tend to be military. These include high-resolution radar systems and electronic countermeasures. Obviously, the availability of data is also limited for security reasons.

There is also a technical difficulty. Both these devices depend for their action on beams of electrons passing, and being modulated by, cavities tuned to the frequency of interest. As the frequency of operation goes up, the cavity size decreases and so the electron beam has to become smaller (and its power carrying capacity therefore decreases). In fact, the power carrying capacity decreases as $1/f^2$. There are obvious ways around this problem, such as creating magnetrons with several anodes in a common evacuated package - but again the extent of these developments are to some extent secret [16]. Experiments with both these generator types, with the aim of increasing their performance at Millimeter Wavelengths, have resulted in devices like the Extended Interaction Klystron [17] and the Space-Harmonic Magnetron [18].

6. 2   Gyrotrons and Hybrid Devices

The Gyrotron is a newer device than either the Klystron or Magnetron and not effected by the $1/f^2$ limitation - this is because it does not have a cavity structure as such. It is, in-fact, a Free-Electron Maser, utilising cyclotron emission to generate its energy [19, 20].

At the start of the 1980s, a number of 60GHz Gyrotrons were reported in the literature; these ranged in power up to 250kW [21, 22]. These early devices were developed particularly by the Hughes Aircraft and Varian companies. Since that time, the technology has advanced considerably, with prototypes delivering 2MW continuous power at 170GHz with efficiencies of 50% or more [23]. This research is being driven by the plasma physics community and currently by the ITER project. The technology of these devices, scaled to 61GHz should be capable of even higher powers and efficiencies.

Hybrid devices, utilising combinations of Gyrotron technology and that of other devices are also starting to appear, although research is still at an early stage. One such design is for a 10MW device operating at 91.4 GHz [24] again designed for plasma physics applications. Another similar design at the University of Maryland yielded 32MW at 19.7GHz. Other, less

detailed designs are available at powers of 100MW [25]. These hybrids are very likely to yield devices useful to EMA with development.

The principle disadvantage of most designs for standard Gyrotrons is their need for high magnetic fields and hence a reliance on superconducting magnets. These add considerably to the complexity and weight of a system. However, these devices have a rather limited range of applications outside particle accelerators and plasma physics, where weight and similar factors are not an issue, and there has been no attempt to design a device for applications such as EMA. The available literature however indicates that the design of such a specific device is likely to be successful.

These issues (along with the reliability of single devices and the other points raised in section 5) point to the use of multiple radiation generators, rather then one large device.

7.   POWER SUPPLY ISSUES

Although there are some practical aspects of EMA, outlined in the preceding sections, which need further development - particularly duct design, loss minimisation and radiation generation; none of these is outside the reach of current technology. The availability of suitable power supplies is the reason why EMA may lie some way in the future. This section reviews a number of ideas about powering EMA. Some of these are a review of existing research and some are the more speculative suggestions of the authors.

As noted in the original paper, of the current technologies, probably only nuclear fission has the capability to provide the power which EMA needs. However, at the time of writing, it is not politically acceptable to allow fission reactors to fly. This was not always the case - and both the USA and USSR flew reactors during the cold war. America studied nuclear power in Aircraft in the Nuclear Energy for the Propulsion of Aircraft (NEPA) project and later in Aircraft Nuclear Propulsion (ANP) and Pluto projects. It even designed a nuclear bomber designated the WS-125. Russia also designed an experimental aircraft, the Tu-119, along similar lines. Both countries flew reactors as part of the test programmes; however, these were not connected to the aircraft propulsion systems. The main difficulty was the heavy nature of the radiation shielding required. Nuclear powered rockets were also extensively explored in the USA [26]. Reactor technology has moved on considerably since these early experiments - particularly in the field of small reactors [27]. However, the obvious concerns and the nuclear industry's poor safety record will remain as an obstacle to any further development.

There are two alternatives to the generation of energy on board the craft. One is to store it in a high energy-density receptacle - a possible method of doing this is described in the next paragraph. The other is to generate the energy elsewhere and transmit it to the vehicle. The two most obvious possibilities for this are delivery upwards, from a ground-based station or downwards from space. Both of these have been explored in theoretical work. Energy transmitted upwards [28], often termed "Beamed Energy Propulsion," has been analysed for powering an engine directly through heating of a propellant or indirectly by collecting and transforming the power into a different form. Microwave systems are those most commonly mentioned in the literature, although optical systems are also described. The disadvantages are mainly the losses associated with atmos-

pheric attenuation. Beaming power downwards, from a space based generator (often a solar collector), has also been theoretically explored [29]. The advantage of this approach, is that the vehicle may be well above most of the atmosphere when power is required and therefore attenuation is lower. However, there is an obvious safety risk of the beam missing its target and damaging assets on the ground.

To turn to the issue of storing energy; one storage medium seems to be particularly promising - that of supercapacitors. These (and ultracapacitors) are energy storage devices operating on the same principles as a normal capacitor, but engineered, commonly using new materials or nanotechnology, to have a very large capacitance. A major advance in the field was reported in the journal *Nature Nanotechnology* this year (2009) [30] and subsequently more widely in the press. The technology has the capability to store a power-density of 1 MW/kg. There are, of course, many obstacles to overcome if similar technologies are to be scaled up to an appropriate size - however, there does not appear to be any physical reason why they should not be.

7.1 Heat Based Generators

If a convenient source of heat can be obtained - either through nuclear means or some other route, then there is a potentially useful way of turning this into electrical power by means of similar technology to that used in the radiation generating devices. Consider Fig, 12.

In this diagram, the cathode is heated by external means - heat from a reactor or from combustion, as outlined in the next section. The cathode is patterned to have a large surface area and emits electrons which are then captured by the anode. The operation of the system is governed by the Richardson-Dushman equation.

$$J = AT^2 e^{-\frac{W}{kT}}$$

Where T is the absolute temperature, W is the material's work function, k is Boltzmann's constant and A is a material-dependent constant. J is the emitted current density. This technology has been used for some time as a method of directly generating electrical energy from heat [31]. The principle is exactly the same as that of the electron gun in the radiation generators themselves and is capable of generating large powers. Obviously, this potentially allows it to be completely integrated with the radiation generating device. The emission efficiency of the cathode is critically dependent on its work function and various materials like Lanthanum Oxide provide high efficiency emission. Cathode fabrication is also undergoing rapid development due to advances in nanotechnology. Techniques such as the micro-patterning of materials and the use of Carbon Nanotubes provide vary large emission areas and high electric-field densities. Devices using similar principles, but in the solid-state, are also under investigation.

The principle drawback of the technique is the lack of high generated voltages (in this form, it produces high current, low voltage, power). The radiation generating devices require high voltages (because electron emission is more efficient if field enhanced - so called "Schottky Emission"). There are several potential ways around this. One is to connect several of the devices in series; this may be simpler than it first seems, because multiple anode-cathode structures can be contained
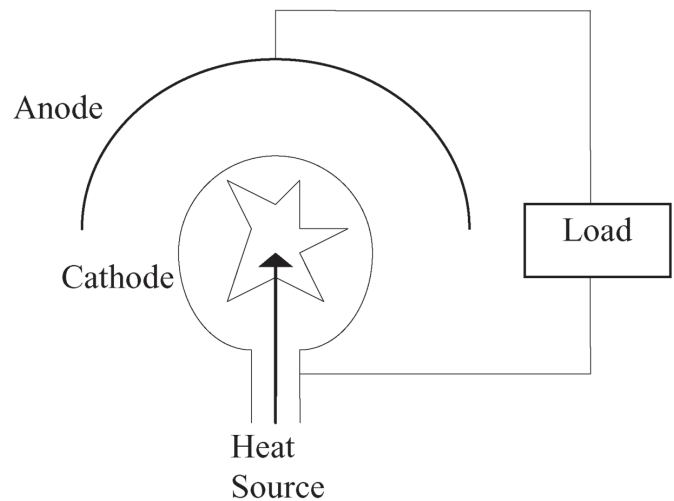

Fig. 12 A thermal-electrical converter.

within the same evacuated envelope. Another approach is to convert the power to alternating current and use a charge pump or a similar impedance transformer. It may be also be possible to use a return-less electrostatic or thermally induced charge to create a high voltage. Obviously, this system also lends itself to combination with the supercapacitors mentioned in the previous section.

7.2 Heat Generation by Combustion

The system outlined above - generating electrical power directly from heat, is well established in theory and practice. The source of heat may be a reactor, as previously outlined. Another option is to use combustion to produce heat.

It might be asked, why should combustion be considered, having been discarded for direct propulsion. The answer to this is that once the requirement for producing thrust has been removed and the sole purpose of the system is the production of heat, several of the issues surrounding combustion are removed or reduced. For example, it may be possible to slow the flow down considerably if the heat thereby generated (which in propulsion scenario would be waste) can be reclaimed. Likewise, duct structures like the Busemann Biplane, which produce no wave-drag (but also no thrust) can be used. Similarly grids or meshes in the duct cross-section, inefficient in thrust systems, can be used for injection, mixing or heat recovery.

Another possible option is to use a swirl or vortex generating structure. This has two possible benefits both related to the increased time of the airflow in the combustor structure. Firstly, it allows more time for mixing and combustion. Secondly it allows time for good heat transfer between the fluid and the duct walls.

In all these scenarios, the cathode of a thermal generating system, similar in principle (but obviously different in detailed topology) would be wrapped around the duct walls, or connected to the duct using a heat exchanger, so as to convert the available heat into electrical energy as outlined. It is hoped to publish a paper with a detailed design study of this approach at some point in the near future.

8.   CONCLUSIONS

The preceding sections cover what might be termed some of the

"second order" effects of EMA, not described in detail in the first paper. Of these issues, the most important from a practical point of view, is that of loss and efficiency.

As is evident from section 5, the largest loss is certainly that caused by reflection and is associated with material resistance. From the figures presented, the design constraints on the duct topology can be seen for the first time. To maximise efficiency, long pathlengths before reflection (and therefore wide ducts) are necessary. High active-species number-densities are also useful. These two constraints help to inform the aerodynamic design of the duct.

Reflecting materials and their temperature control also play an important role in reducing losses. Particularly the use of high reflectivity mirrors, kept cool by mechanical design, careful selection of duct profile and perhaps active cooling. These are among the considerations which make it likely that several small radiation sources are used, rather then a single large one.

These constraints need the application of some ingenuity to maximise performance. Since reflection and (to a lesser extent) window losses increase with frequency; one further idea mentioned in the first paper is certainly worth further study. This may reduce the operating frequency of the system considerably and in turn allow the use of simpler, more efficient, generating devices. The concept was to inject another material into the flow and activate this. If the material can be activated at lower frequency than that considered here (and many can) and has a high absorption (again, which many have), then the advantages

of doing this might outweigh the obvious disadvantages. The usual problems with stoichiometric mixing of the material into the flow do not apply, since we are not trying to burn the material. It is hoped that a paper considering this approach may be published in the medium term.

Currently, there are few devices available for signal generation, due to the limited number of high-power applications in this part of the millimeter wavelengths. However, suitable devices have been run experimentally and there is no physical reason why such devices may not be further developed. It seems likely that the efficiency of these will be in the region of 45-60%. This makes it a reasonably informed guess that the efficiency of the whole system will be between 20% and 40% depending on Mach number and the overall design used. This figure does not include the power supply system.

As was explained in the first paper, the power supply is that part of the system which seems outside the reach of current technology. Of course, as explained earlier, nuclear supplies could fulfil the task, but development of these seems unlikely at present. The suggestions made in the section on power supplies are speculative, but are included in order to encourage discussion and debate on the alternatives.

In conclusion, it is hoped that this paper will add to the initial description of the system previously published, answer some of the outstanding questions about efficiency and practical design and serve as a point of discussion for those interested in exploring this technique further.

REFERENCES

1. C. MacLeod, "Electromagnetically Activated Hypersonic Ducts", *JBIS*, **62**, pp.99-109, 2009.
2. F.S. Billig, "Design and development of single stage to orbit vehicles", *John-Hopkins Applied Physics Laboratory Technical Digest*, **11**, pp.336-352, 1990.
3. J.D. Anderson, "*Fundamentals of aerodynamics (3rd ed)*", McGraw-Hill, New York, pp.538-542, 2001.
4. J.E. John, "*Gas Dynamics (2nd Ed)*", Allyn and Bacon Inc, Boston, pp.338-349, 1984.
5. W.H Heiser *et al*, "Hypersonic Airbreathing Propulsion", *AIAA Education Series*, Washington, 1994.
6. R. Meredith, "*Engineer's Handbook of Industrial Microwave Heating*", IEE, New York, 1998, p.56.
7. E.T. Curran and S.N.B. Murthy, "Scramjet Propulsion", in *Progress in Astronautics and Aeronautics* (Series V-189), AIAA, Washington, 2001.
8. S. Ramo, J.R. Whinnery and T. Van Duzer, "*Fields and Waves in Communication Electronics (3rd ed)*". Wiley, New York, pp.145-155, 286-315, 1994.
9. G. Ghosh, J. Miyake and M.E. Fine, "The systems-based design of high-strength, high conductivity alloys", *The JOM Journal of Minerals, Metals and Materials Society*", **49**, pp.56-60, 2008.
10. Z. Castro-Dettmer, C. Persad, "Performance of a Copper-Silver Alloy as an Electromagnetic Launcher Conductor Material", *IEEE Transactions on Magnetics*, **41**, pp.176-181, 2005.
11. L.A. Gorelov *et al*, "Diamond Gyrotron Windows at the DIII-D Tokamak", *Infrared and Millimeter waves - The 13th International Conference on Tetrahertz Electronics 2005 (IRMMW-THz 2005)*, **2**, pp.357-358, 2005.
12. S.J. Zinkle and R.H. Goulding, "Loss Tangent Measurements on Unirradiated Alumina," Oak Ridge National Laboratory, 1996, Report number ORNL/M-5023, also available as OSTI report number DE96010874, pp.231-235.
13. R. Sturdivant, "Millimeter-Wave Performance of Alumina High Temperature Cofired Ceramics IC Packages", *The 39th International Symposium on* Microelectronics (IMAPS 2006), 2006.
14. P.P. Woskov and C.H. Titus, "Graphite Millimeter-wave Waveguide and Mirror for High Temperature Environments", *IEEE Transactions on*

Microwave Theory and Techniques*, **43**, pp.2684-2688, 1995.
15. M.Y. Tretyakov *et al*, "60-GHz oxygen band: precise broadening and central frequencies of fine-structure lines, absolute absorption profile at atmospheric pressure and revision of mixing coefficients", *Journal of Molecular Spectroscopy*, **231**, pp.1-14, 2005.
16. R.E. Collins, "*Foundations for Micowave Engineering (2nd ed)*", McGraw-Hill, New York, pp.648-712, 1992.
17. B. Steer *et al*, "Advantages of extended interaction klystron technology at millimeter wave frequencies", *The Pulsed Power Plasma Science Conference (PPPS 2007), IEEE*, **2**, pp.1049-1053, 2007.
18. O.P. Kulagin and V.D. Yeryomka, "The flow forming potential in unconventional magnetrons", *Vacuum Electronics Conference (IVEC 2004), IEEE*, pp.224-225. 2004.
19. G.S. Nusinovich, "*Introduction to the Physics of Gyrotrons*", The John Hopkins University Press, Baltimore, 2004.
20. M.V. Kartikeyan, E. Borie and M. Thumm, "*Gyrotrons: High-power Microwave and Millimeter Wave Technology*", Springer, New York, 2003.
21. M. Caplan *et al*, "Test results of 96 GHz, 10 kW Gyrotron and a 60 GHz, 200 kW Gyrotron", *The International Electron Devices Meeting (IEDM 81)*, pp.188-189, 1981.
22. W. DeHope *et al*, "250kW high efficiency Gyrotron oscillator operating at 60 GHz", *The International Electron Devices Meeting (IEDM 82)*, 1982, pp. 366 - 367.
23. B. Piosczyl *et al*, "A 2MW, 170GHz coaxial cavity gyrotron - experimental verification of the design of main components", *The third IAEA technical meeting on ECRH physics and technology in ITER*, pp.24-32, 2005.
24. W. Lawson *et al*, "Design of a 10-MW, 91.4GHz frequency-doubling GyroKlystron for advanced accelerator applications", *IEEE Transactions on Plasma Science*, **29**, pp.545-558, 2001.
25. M. Castle *et al*, "An overmoded coaxial buncher cavity for a 100-MW gyroklystron", *IEEE Microwave guided wave letters*, **8**, pp.302-304, 1998.
26. J.A. Dewar, "*To the end of the Solar System: The story of the nuclear rocket (2nd ed)*", Apogee books, Burlington, 2008.
27. P. McKenna, "Are 'disposable' reactors a safe energy solution", *New*

Scientist, **2667**, pp.34–37, 2008.

28. Y. Oda *et al*, "An Experimental Study on a Thrust Generation Model for Microwave Beamed Energy Propulsion", *The 44th AIAA Aerospace Sciences Meeting and Exhibit*, pp.1-7, 2006.

29. P. Koert and J.T. Cha, "Millimeter Wave Technology for Space Power Beaming", *IEEE Transactions on Microwave Theory and Techniques*, **40**, pp.1251-1258, 1992.

30. P. Banerjee *et al*, "Nanotubular metal-insulator-metal capacitor arrays for energy storage", *Nature Nanotechnology*, **4**, pp.292-296, 2009.

31. A.V. da Rosa, "*Fundamentals of Renewable Energy Processes*", Elsevier Academic Press, Burlington, pp.199-240, 2005.

*   *   *